Supplementary Information

An Autonomous Microreactor Platform for the Rapid Identification of Kinetic Models

Conor Waldron, Arun Pankajakshan, Marco Quaglio, Enhong Cao, Federico Galvanin, Asterios Gavriilidis
Department of Chemical Engineering, University College London, London, WC1E 7JE, U.K.

Contents

1. Estimation of Density, Viscosity and Diffusion Coefficients

In assessing the flow, mixing and heat transfer characteristics of the reactor the values of the various physical properties, such as density and viscosity, were taken as the values of pure ethanol. The feed solution was 10% by volume sulfuric acid in water (catalyst) and 90% by volume benzoic acid in ethanol (ranging from 0.9 to 1.55 M benzoic acid concentration), therefore the feed solution consisted of approximately 70-75% ethanol, 15-20% benzoic acid and 10% water by mass. Neglecting the presence of water and benzoic acid is not expected to significantly affect the results and it will be shown later that even if worst-case scenario estimates are made, the system still behaves as desired, with plug flow behaviour and fast heat transfer. The viscosity, μ, and density, ρ, of pure ethanol at a range of temperatures was taken from the Dortmund Data Bank[1, 2] and are shown in Figure S1 below. The viscosity (mPa·s) of ethanol can be obtained from the Vogel equation, (Eq S1), with the parameters from the Dortmund Data Bank[3] and temperature in Kelvin. A polynomial expression is fitted to the experimental density values obtained from the Dortmund Data Bank, (Eq S2), where temperature is in Kelvin and density is in kg/m^3.

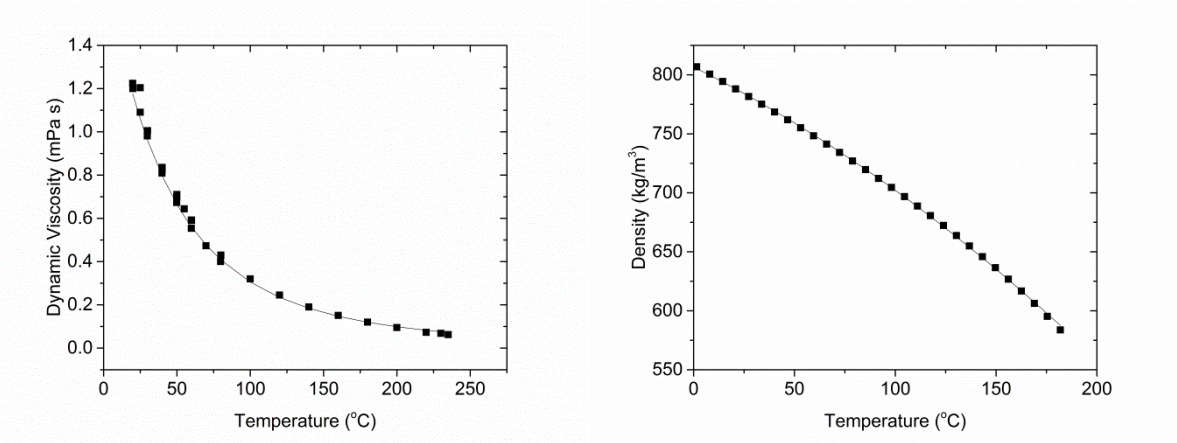

Figure S1. Dynamic viscosity and density of ethanol as a function of temperature, taken from the Dortmund Data Bank.

$$\mu = \exp\left(-7.3714 + \frac{2770}{74.6787 + T}\right) \quad \text{(Eq S1)}$$

$$\rho = -0.0019413\,T^2 + 0.20877\,T + 894.471 \quad \text{(Eq S2)}$$

The Wilke-Chang empirical equation is often used to estimate the value of the molecular diffusion coefficient for systems where the solute and solvent molecules are approximately the same size. The Wilke-Chang equation for the diffusion coefficient (in cm^2/s) is [4]

$$D_m = \frac{7.4 * 10^{-8}(\varphi M_2)^{0.5} T}{\mu_2 V_1^{0.6}} \quad \text{(Eq S3)}$$

where subscripts 1 and 2 are for the solute and solvent respectively, φ is the association parameter of the solvent, which is 1.5 for alcohols, M is the molecular weight (g/mol), μ is the viscosity (centipoises), V is the molar volume (ml/mol) and T is the temperature (K). This equation is only valid in dilute solutions.[4] This is a reasonable assumption, as the concentration of benzoic acid (0.9 -1.55 M) was low compared to the concentration of the ethanol solvent (typically 13 - 15 M). For benzoic acid in ethanol the molecular weight of the solvent is 46.07 g/mol, the molar volume of benzoic acid

is 92.5 mL/mol and the density and viscosity exhibit a temperature dependence described above. Using these values, the molecular diffusion coefficient of benzoic acid in ethanol as a function of temperature was calculated and shown in Figure S2.

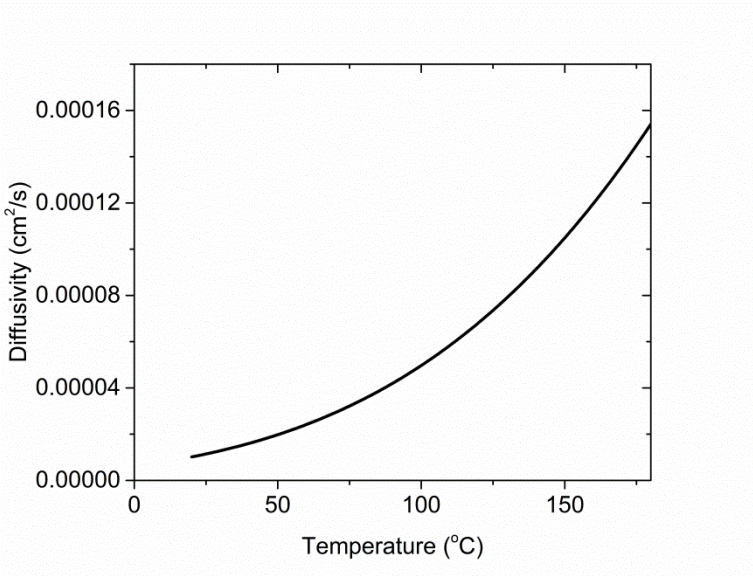

Figure S2. Molecular diffusion coefficient of benzoic acid in ethanol, calculated using the Wilke-Chang equation.

2. Reactor Hydrodynamics

The small reactor diameter of 250 μm was chosen to ensure plug flow behaviour as demonstrated below, while the long reactor length of 2 m was required to provide a suitable reactor residence time to produce a reasonable rate of reaction at the range of flowrates desired. Flowrates used in this work varied in the range 5-100 μL/min. The reactor is shown to behave as plug flow reactor with only small dispersion. This is based on the calculation of the vessel dispersion number, N_L

$$N_L = \frac{1}{Pe_L} = \frac{D_{ax}}{uL} \quad \text{(Eq S4)}$$

where D_{ax} is the axial dispersion coefficient (m^2/s), u is the average velocity (m/s) and L is the length (m). The commonly used criterion for plug flow is to have a vessel dispersion number below 0.01.[5] The vessel dispersion number is the inverse of the Peclet number, Pe_L. The axial dispersion coefficient, D_{ax}, was calculated using the Aris expression, Eq S5, where d_t is the tube diameter (m) and D_m is the molecular diffusion coefficient (m^2/s).

$$D_{ax} = D_m + \frac{u^2 d_t^2}{192\, D_m} \quad \text{(Eq S5)}$$

The validity of plug flow was assessed at 100 ^oC, where the values of density, viscosity and molecular diffusion coefficient are 702 kg/m^3, 0.3054 mPa·s and $4.97*10^{-5}$ cm^2/s. The validity of the axial dispersion model was confirmed by examining the reactor operating point on a map given by Levenspiel,[5] where the operating point is determined by the Bodenstein number and the length to diameter ratio of the reactor. The Bodenstein number was calculated from

$$Bo = Re * Sc = \frac{\rho u d_t}{\mu}\frac{\mu}{\rho D_m} = \frac{u d_t}{D_m} \quad \text{(Eq S6)}$$

For the lowest and highest flowrates considered (5 and 100 μL/min) Bodenstein numbers of 85 and 1708 were calculated. As the length to diameter ratio was 8000, the reactor operated in the "axial dispersion model" region.[5] The axial dispersion coefficient was calculated to range from $1.9*10^{-7}$ to $7.5*10^{-5}$ m^2/s using the Aris expression (Eq S5). With this range of axial dispersion coefficients, the vessel dispersion number was found to range from $5.7*10^{-5}$ to 0.001 for flowrates from 5 to 100 μL/min. The vessel dispersion number was significantly lower than the criterion for small deviation from plug flow of 0.01, hence verifying that the reactor exhibited plug flow behaviour. This calculation was repeated at room temperature, where density, viscosity and molecular diffusion coefficient are 789 kg/m^3, 1.176 mPa·s and $1.01*10^{-5}$ cm^2/s. In this case, at the lower and upper flowrates of 5 and 100 μL/min, the vessel dispersion number was $2.77*10^{-4}$ and 0.0055, which are still within the plug flow limits.

3. Mixing Characteristics of the System

It is important that the reagents were completely mixed before entering the reactor. The flowrates used were very low with Reynolds numbers less than 10, resulting in laminar flow. The mixing was then modelled as mixing by molecular diffusion in shear flow, as described by

$$t_{mix} = A\frac{R^2}{D_m} \quad \text{(Eq S7)}$$

$$A = \frac{1}{(1+p)(3+p)} \quad \text{(Eq S8)}$$

where R is the half thickness of the fluid, D_m is the molecular diffusivity and A is the shape factor given by Eq S8, where p equals 0, 1 and 2 for a slab, cylinder and sphere respectively.[6] To estimate the mixing time required for benzoic acid in 250 μm tube diameter, Eq S7-S8 were used with half thickness R = 125 μm, p = 1 for a cylindrical geometry, and the molecular diffusivity of benzoic acid in ethanol at room temperature $1.01*10^{-5}$ cm^2/s. The mixing time was calculated to be 1.95 s, which even for the highest flowrate of 100 μL/min, results in a mixing length of 6.6 cm. As the length of tubing between the mixing point and the start of the reactor was 30 cm long, complete mixing of reagents was achieved before the reactor inlet.

4. Heating Characteristics of the Reactor

The reactor volume was defined as the volume of tubing that was submerged in the oil bath and was hence at the reaction temperature. This requires the assumption that the reaction fluid heated up instantaneously from room temperature to the oil bath temperature as soon as it passed the point of submersion, and also that it cooled instantaneously from the oil bath temperature to room temperature at the point where the tubing exited the oil bath.

The rate of heat flow needed, Q (J/s), to increase the reaction fluid temperature from room temperature, T_{room} (K), to the oil bath temperature, T_{bath} (K), is given by [7]

$$Q = mC_{p\ EtOH}(T_{bath} - T_{room}) \quad \text{(Eq S9)}$$

where $C_{p\ EtOH}$ (J/kg·K) is the specific heat capacity of ethanol (assumed to be 2440 J/kg·K [8]) and m (kg/s) is the mass flowrate of reaction fluid (assumed to be pure ethanol). The worst case scenario was heating ethanol from 25 °C to 140 °C. The fastest flowrate used in steady state experiments was 20 µL/min and the fastest flowrate used in transient experiments was 100 µL/min. For these two scenarios the heat flow required, calculated from Eq S9, was 0.07 and 0.38 W.

The heat exchange area, A (m^2), required to achieve this temperature difference is calculated using

$$Q = UA\Delta T_{LM} \quad \text{(Eq S10)}$$

where U is the overall heat transfer coefficient (W/m²·K) and ΔT_{LM} is the log mean temperature difference (K) [7, 9]. It is not possible to use the oil bath temperature as the outlet temperature, since this required an infinite heat transfer area, hence a value 0.1 °C lower was used. The log mean temperature difference was calculated to be 16.3 °C using Eq S11.

$$\Delta T_{LM} = \frac{(T_{bath} - T_{in}) - (T_{bath} - T_{out})}{ln\left(\frac{T_{bath} - T_{in}}{T_{bath} - T_{out}}\right)} \quad \text{(Eq S11)}$$

U is found from the sum of the three heat resistances, convection within the reactor, conduction through the tube and convection outside the tube. [7, 9]

$$\frac{1}{U} = \frac{1}{h_i} + \frac{d_i}{2k_t} ln\left(\frac{d_o}{d_i}\right) + \frac{d_i}{d_o h_o} \quad \text{(Eq S12)}$$

where h_i is the heat transfer coefficient (W/m²·K) inside the tube, d_i and d_o are the inner and outer diameters of the reactor tube, which had values of 0.00025 m and 0.00158 m respectively, k_t is the thermal conductivity of the PEEK reactor tubing (0.25 W/m·K) and h_o is the heat transfer coefficient (W/m²·K) on the outside of the tube. The inner heat transfer coefficient was found from the Nusselt number calculated using the empirical correlation for laminar flow in tubes shown in Eq S14 [7, 9]

$$Nu = \frac{h_i d_i}{k_{EtOH}} \quad \text{(Eq S13)}$$

$$Nu = 1.86\left(RePr\frac{d_i}{L}\right)^{1/3}\left(\frac{\mu}{\mu_w}\right)^{0.14} \quad \text{(Eq S14)}$$

where Pr is the Prandtl number, L is the tubing length and μ and μ_w are the viscosity of the fluid in the bulk and the wall respectively. In this work, a very low Nusselt number of less than 1 was calculated. However, if a Nusselt number of less than 3.5 is calculated, then a value of 3.5 should be

used.[9, 10] From the Nusselt number the internal heat transfer coefficient of 2400 W/m^2·K was calculated from Eq S13, where k_{EtOH} is the thermal conductivity of ethanol (0.171 W/m·K).[11]

The outer heat transfer coefficient for the tube in the glycerol filled agitated oil bath was estimated from empirical correlations. The correlation for a six-bladed impeller in a fully baffled vessel was used, as shown in Eq S15. While the small oil bath used in this work is not a fully baffled vessel with a six-blade impeller, only order of magnitude accuracy was needed for these calculations.

$$\frac{h_o d_o}{k_{EtOH}} = 0.17 \left(\frac{\rho N d_{imp}^2}{\mu}\right)^{0.67} \left(\frac{C_{p\,EtOH}\mu}{k_{EtOH}}\right)^{0.37} \left(\frac{d_o}{d_v}\right)^{0.5} \quad \text{(Eq S15)}$$

In Eq S15, N is the number of rotations per second (which was 10 from the hot plate stirrer set point), d_{imp} is the diameter of the impeller (0.03 m) and d_v is the diameter of the vessel (0.1 m). The physical properties of glycerol were taken from the literature.[12, 13] At 140 °C glycerol has a density of 1187 kg/m^3, a viscosity of 0.0051 Pa·s, a specific heat capacity of 270 J/kg·K and a thermal conductivity of 0.285 W/m·K. Using these values, the outer heat transfer coefficient was estimated to be 1678 W/m^2·K.

Combining the values for the conductivity of the reactor wall k_t with the internal and external heat transfer coefficients (2400 and 1678 W/m^2·K), the overall heat transfer coefficient was 690 W/m^2·K. Using Eq S10, the area and hence length of tubing required for heating was calculated for the fastest flowrate used in steady state experiments of 20 µL/min; only 0.8 cm of tubing was required, which can be considered negligible compared to the 2 m reactor length. For the fastest flowrate used in transient experiments the length of tubing required was 4 cm. This larger value is still considered negligible, as it is only 2% of the reactor length.

The length of tubing required to cool the reaction fluid was calculated in the same way, except an external heat transfer coefficient of 10 W/m^2·K was chosen, as a typical value for natural convection in air around a tube.[14] This gave an overall U value of 59 W/m^2·K, showing that cooling was slower. However, the objective here was not to cool back down to room temperature, but to quench the reaction. Since the reaction is effectively quenched at 60 °C it was only necessary to cool to this value. The log mean temperature difference was then calculated to be 67 °C and the required cooling length for the fastest steady state experiment of 20 µL/min flowrate was only 1.6 cm, which could be considered negligible. For the fastest transient experiment of 100 µL/min flowrate the required cooling length was 8 cm, which corresponds to 4% of the reactor length. This was small enough to be neglected.

These calculations indicate that it was reasonable to assume the reactor heats up and cools down instantly upon entering and leaving the oil bath, especially for the steady state experiments and hence the reactor volume could be calculated as the tube volume submerged in the oil bath.

5. Parameter Estimation Accuracy and Precision

As discussed in the main text, parameter estimates are themselves random variables with their own probability distribution function. The two most important quantities used to describe a parameter estimate are its accuracy and its precision. A graphical demonstration of accuracy and precision is shown in Figure S3, where the probability distribution function of two estimates for the same parameter are shown along with the true parameter value, which for this example is assumed to be known. Accuracy is how close the mean parameter value is to the true parameter value. In this case, the blue-dash parameter estimate has a very high accuracy, as the mean parameter value and the true parameter value overlap. In comparison, the solid red curve corresponds to a parameter estimate with low accuracy. Precision is a measure of spread or variance in the parameter estimate. As parameter estimates are random variables, every time an identical experimental campaign is repeated and parameter estimation is performed a new parameter estimate is obtained. Precision then gives an indication of how far apart repeated parameter estimates are. In Figure S3 the blue-dash curve has a low precision, while the solid red curve has a high precision. Unfortunately, in most experimental work the true parameter value is not known, so it is only possible to measure precision.

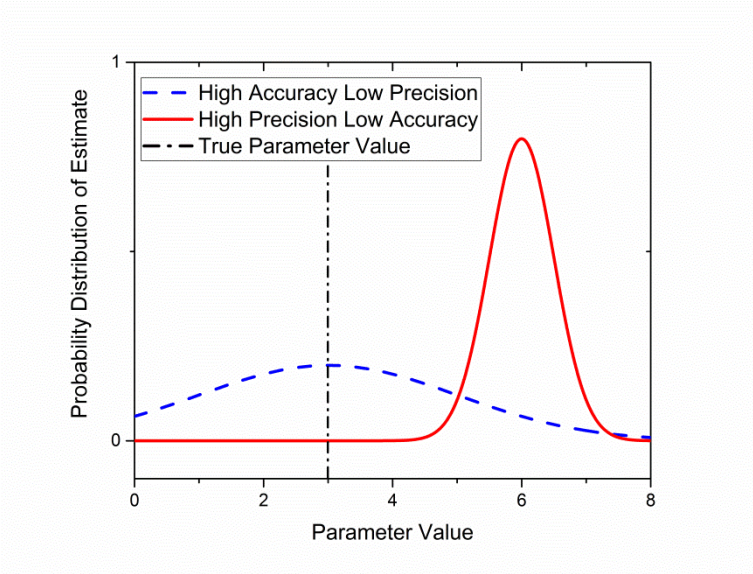

Figure S3. Graphical demonstration of accuracy and precision in parameter estimation.

6. Dead Volume Correction

The dead volume correction is derived by equating the dead volume, V_{dead}, to the integral of flowrate, v, from the time the sample left the reactor, t_L, to the time the sample was injected to the HPLC, the measurement time, t_M, as shown in Eq S16. The dead volume and the measurement time are known, so Eq S16 can be used to solve for the unknown time t_L.

$$V_{dead} = \int_{t_L}^{t_M} v\, dt \qquad \text{(Eq S16)}$$

In all the transient experiments conducted the flowrate was ramped at a constant ramp rate. Therefore, the flowrate can be expressed by

$$v = v_0 - \alpha t \qquad \text{(Eq S17)}$$

where v_0 is the initial flowrate and α is the rate of decrease of the flowrate. Substituting Eq S17 in Eq S16 and integrating leads to the quadratic equation

$$\left(\frac{1}{2}\alpha\right) t_L^2 - (v_o) t_L + \left(v_0 t_M - \frac{1}{2}\alpha t_M^2 - V_{dead}\right) = 0 \qquad \text{(Eq S18)}$$

Solving this equation leads to only one physically meaningful solution shown in Eq 19 in the main text, also shown below

$$t_L = \frac{v_0 - \sqrt{v_0^2 - 4 * \frac{\alpha}{2} * \left[v_0 t_M - \frac{\alpha}{2} t_M^2 - V_{dead}\right]}}{\alpha} \qquad \text{(Eq 19)}$$

The t_L was calculated using the measured 44.2 µL dead volume between the reactor outlet and the HPLC sample loop. Note that it is possible to calculate, t_{In}, the time a fluid element entered the reactor by replacing V_{dead} in Eq 19 with the sum of V_{dead} and V_{Rxr}, the reactor volume. Then it is possible to calculate the residence time of each sample, τ, by subtracting t_{In} from t_L

$$\tau = t_L - t_{In} \qquad \text{(Eq S19)}$$

7. LabVIEW Code

Two separate LabVIEW codes were developed, one for the design of a campaign of steady-state experiments and one for the design of transient experiments. The LabVIEW code consists of a “block diagram” and a “front panel”. The block diagram is where the code is written, while the front panel is meant to be a user-friendly interface to allow any user to operate the LabVIEW program. The front panel is where the user provides information to LabVIEW, such as the feed concentration in the syringes. The front panel for the steady-state experiments is shown in Figure S4. On the left hand side of the front panel, the current process variables are reported as numbers as well as visually in graphs. The LabVIEW code records all process variables every 5 s in an Excel file to allow the user to check at a later time that the experiments were performed correctly. Also on the left hand side are two toggle switches, the first is for selecting to either run an automated campaign of experiments or to manually control all set points. If the user chooses to run an automated campaign, where LabVIEW will conduct multiple experiments, the user must specify on the second toggle switch if the campaign will use a list of pre-selected experimental conditions or if the user wants to run a MBDoE campaign. The MBDoE criteria is chosen by entering “A”, “D” or “E” in the “MBDoE Criteria” text field. In the centre of the front panel there is a section labelled “Pre-planned Experiments” which is activated when the user selects to run a list of pre-selected experiments. In this area, the user enters the values of temperature, total flowrate and concentration for the 8 experiments that will be automatically performed by the system. The LabVIEW code shown was written to conduct campaigns of 8 experiments, as this required 8 h and could be completed during normal working hours. However, the code can be easily extended to include any number of experiments. Also in the centre of the front panel is the “MBDoE Experiments” section, where during an MBDoE campaign the experimental conditions are shown as they are designed by the Python MBDoE algorithm. On the right of the front panel there is a section labelled “Measured Concentrations”, where the steady-state outlet concentration of benzoic acid and ethyl benzoate are shown for each experiment, after the experimental duration has been reached. Finally, on the extreme right of the front panel is the “Online Parameter Estimates” section, where the results of online parameter estimation are reported including parameter estimates, χ^2 values, t-values and confidence intervals. Additionally, the LabVIEW code includes safety shutdown features, shown on the far left of the front panel, that will safely turn off all equipment if a given temperature or pressure is exceeded or if a syringe is emptied. For running automated experiments it is necessary to provide LabVIEW with information about the experiments, such as the concentrations in the low and high concentration benzoic acid syringes, the desired duration of an experiment and the volumetric fraction of sulfuric acid. This information is given to LabVIEW through the front panel under the “Experimental Info” section. It is also possible to have direct user control, where the user sets the flowrates of each syringe and chooses the temperature set point directly. For direct user control, the user inputs these values in the “Manual Control” section.

Figure S4. LabVIEW user interface (front panel) for the steady-state experiments.

LabVIEW is a graphical programming language where programmes are not written as lines of code but instead are drawn as flowsheets with logic and loop structures. A simplified version of the LabVIEW block diagram used for the steady state experiments is shown in Figure S5 illustrating how online MBDoE can be achieved by combining *timed* loops, *for* loops, *while* loops and *case structures*. The central component of the LabVIEW code is a *while* loop, which contains a *timed* loop and also a *case structure*. In LabVIEW a *timed* loop repeats a given set of commands at a given frequency until a time limit is reached. In our case, commands were executed every 5 s and the time limit was the experimental duration, which was specified by the user. A *case structure* is the LabVIEW equivalent of an "if, else-if, else" logic structure, and this is used in Figure S5 to allow different commands to be given for different experiments. To assist the reader understanding the LabVIEW code, the algorithm is also explained in Table S1.

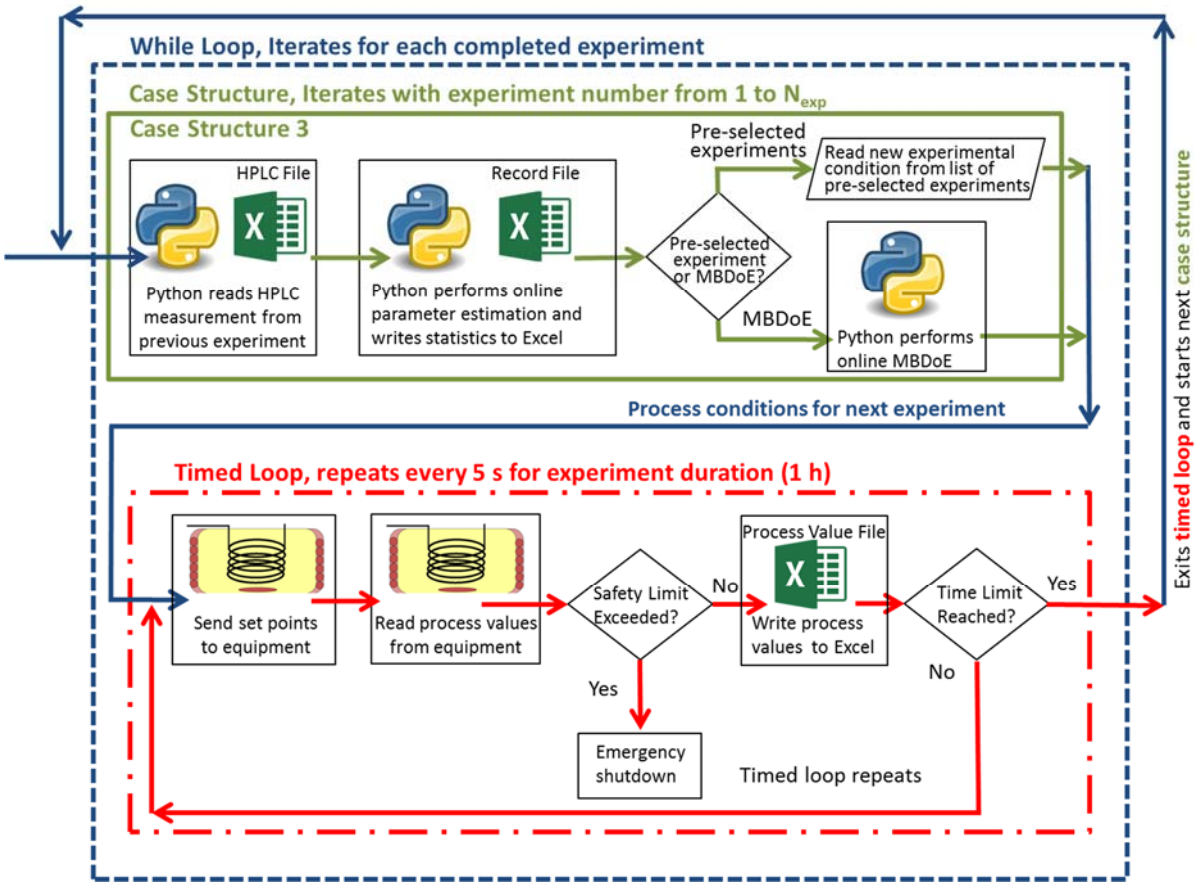

Figure S5. Simplified LabVIEW block diagram showing the major flows of information and decision making.

Table S1. The algorithm applied in the LabVIEW code for the automated steady-state campaigns.

Step	Activity	Task in flow chart
1	Read the 1st set point values from the user input fields and send these values to the relevant process equipment.	Case Structure 1 (not shown in Figure S5 due to space limitations)
2	While waiting for the experiment duration, the following tasks are completed every 5 s: • Read the process values. • Compare process values to the safety shutdown values (if values are exceeded the safety shutdown procedure is triggered). • Record the process values in an Excel spreadsheet.	Timed Loop
3	When the experiment duration (specified by user) is reached, the 1st experiment ends and the following commands are carried out: • Using Python read the most recent HPLC values from the HPLC Excel file and store these values along with their corresponding experimental conditions. Note that the HPLC is not controlled by LabVIEW, but is continuously sampling every 7 min and recording the results in the HPLC Excel file. • Read the 2nd set point values from the user input field and	Case Structure 2 (not shown in Figure S5 due to space limitations)

	send these values to the relevant process equipment.	
4	While waiting for the experiment duration, the following tasks are completed every 5 s: • Read the process values. • Compare process values to the safety shutdown values (if values are exceeded the safety shutdown procedure is triggered). • Record the process values in an Excel spreadsheet.	Timed Loop
5	When the experiment duration (specified by user) is reached, the 2nd experiment ends and the following commands are carried out: • Using Python read the most recent HPLC values from the HPLC Excel file and store these values along with the corresponding experimental conditions. • Using Python perform parameter estimation using all previously collected data and record the estimate values and corresponding statistics on the screen and in an Excel file. • If "MBDoE" is selected, using Python perform MBDoE to calculate the experimental conditions for the next experimental conditions and send these values to the relevant process equipment. • If "Pre-selected Experiments" is selected, read the next set point values from the user input field and send these values to the relevant process equipment.	Case Structure 3-8 (case structures 3-8 were identical)
6	Steps 4 and 5 are repeated for the 4th to N_{exp}th experimental conditions.	Timed Loop & Case Structures 3 to N_{exp}
7	When the N_{exp}th experiment ends, the following commands are carried out: • Using Python read the most recent HPLC values from the HPLC Excel file and store these values along with the corresponding experimental conditions. • Using Python perform parameter estimation using all previously collected data and record the estimate values and corresponding statistics on the screen and in an Excel file. • Send the syringe pumps a command to stop pumping and shut down. • Send the heater a command to turn off.	Case Structure N_{exp}+1 (not shown in Figure S5 due to space limitations)

8. Results from Steady-State Factorial Campaigns

Each factorial campaign consisted of 8 individual steady-state experiments where flowrate, temperature and feed concentration were altered. The steady-state outlet concentrations for each experiment in these two identical campaigns, SSF1 and SSF2, are shown below in Table S2 along with the conversion and mole balance. The mole balance is the percentage deviation between the inlet feed concentration and the sum of the outlet benzoic acid and ethyl benzoate concentrations, shown below

$$Mole\ Balance\ \% = 100 * \frac{C_{BA,in} - C_{BA,out} - C_{EB,out}}{C_{BA,in}} \quad \text{(Eq S20)}$$

Table S2. Experimental conditions, benzoic acid conversion, outlet concentrations of benzoic acid (BA) and ethyl benzoate (EB) and mole balance for the Steady-State Factorial campaign 1 (SSF 1) and 2 (SSF 2).

Exp	Temp.	Flowrate	Feed Conc. BA	Conversion		Outlet Conc. BA		Outlet Conc. EB		Mole Balance	
	°C	µL/min	M	%	%	M	M	M	M	%	%
				SSF 1	SSF 2	SSF 1	SSF 2	SSF 1	SSF 2	SSF 1	SSF 2
1	140.0	20	1.5	24.0	24.7	1.14	1.13	0.39	0.36	-2.0	0.7
2	140.0	20	1.0	30.0	23.0	0.70	0.77	0.27	0.25	3.0	-2.0
3	140.0	10	1.5	45.3	41.3	0.82	0.88	0.61	0.64	4.7	-1.3
4	140.0	10	1.0	42.0	43.0	0.58	0.57	0.42	0.43	0.0	0.0
5	120.0	10	1.5	18.0	15.3	1.23	1.27	0.23	0.24	2.7	-0.7
6	120.0	10	1.0	16.0	17.0	0.84	0.83	0.16	0.16	0.0	1.0
7	120.0	20	1.5	8.0	8.7	1.38	1.37	0.13	0.12	-0.7	0.7
8	120.0	20	1.0	9.0	9.0	0.91	0.91	0.08	0.08	1.0	1.0

9. Results from Steady-State MBDoE Campaigns

Each MBDoE campaign consisted of 8 individual steady-state experiments defined by the flowrate, temperature and feed concentration used. The first two experiments were selected in advance by the user, while experiments numbered 3 to 8 were designed by online MBDoE. The values of the temperature, flowrate and feed concentrations designed for each experiment, the benzoic acid conversion, the measured outlet concentrations and the results of online parameter estimation are shown in Table S3 and Table S4 for the D- and E-Optimal MBDoE campaigns respectively. The statistics shown for the parameter estimation are the parameter estimates for KP1 and KP2, as well as the χ^2value with the corresponding 95% χ^2reference value.

Table S3. Experimental conditions, benzoic acid conversion, outlet concentrations of benzoic acid (BA) and ethyl benzoate (EB), kinetic parameter estimates and statistics for the Steady-State MBDoE D-Optimal campaign.

Exp	Temp.	Flowrate	Feed Conc. BA	Conversion	Outlet Conc. BA	Outlet Conc. EB	KP1	KP2	X2	X2 ref
	°C	µL/min	M	%	M	M				
1	140.0	20	1.5	22.7	1.16	0.36	-	-	-	-
2	120.0	10	1.0	15.0	0.85	0.16	9.10	7.80	0.43	8.76
3	119.1	7.5	1.55	16.8	1.29	0.30	9.16	7.99	1.60	12.8
4	140.0	7.5	1.55	50.3	0.77	0.83	9.19	8.26	4.49	16.2
5	116.6	7.5	1.55	14.2	1.33	0.26	9.17	8.20	5.82	19.5
6	140.0	7.5	1.55	50.3	0.77	0.81	9.17	8.15	6.70	22.6
7	117.3	7.5	1.55	14.2	1.33	0.28	9.16	8.13	9.98	25.5
8	140.0	7.5	1.55	51.0	0.76	0.82	9.16	8.14	10.9	28.4

Table S4. Experimental conditions, benzoic acid conversion, outlet concentrations of benzoic acid (BA) and ethyl benzoate (EB), kinetic parameter estimates and statistics for the Steady-State MBDoE E-Optimal campaign.

Exp	Temp.	Flowrate	Feed Conc. BA	Conversion	Outlet Conc. BA	Outlet Conc. EB	KP1	KP2	X2	X2 ref
	°C	µL/min	M	%	M	M				
1	140.0	20	1.5	22.0	1.17	0.37				
2	120.0	10	1.0	14.0	0.86	0.16	9.16	8.13	1.52	8.76
3	112.8	7.5	1.55	11.6	1.37	0.21	9.17	8.19	2.23	12.8
4	112.4	7.5	1.55	12.3	1.36	0.20	9.17	8.19	2.26	16.2
5	140.0	7.95	1.55	47.7	0.81	0.78	9.17	8.11	3.82	19.5
6	114.4	7.5	1.55	12.3	1.36	0.23	9.16	8.09	5.01	22.6
7	113.4	7.5	1.55	12.9	1.35	0.21	9.16	8.10	5.16	25.5
8	114.0	7.5	1.55	12.3	1.36	0.22	9.17	8.12	6.23	28.4

10. Results from Single-Variable Transient Campaigns

The results obtained from the two different single-variable transient experiments are shown in Table S5 and Table S6, along with the time at which the measurement was taken, t_M, the time that the sample left the reactor outlet, t_L, the time the sample entered the reactor, t_{In}, and the sample residence time, τ. The measured outlet concentrations along with the times the samples left the reactor were used for parameter estimation.

Table S5. Time each sample was measured, left and entered the reactor and corresponding residence time, along with conversion and outlet concentrations of benzoic acid and ethyl benzoate for the Single-Variable Transient campaign. Initial flowrate was 100 µL/min, the flowrate was ramped down at a rate of 1 µL/min^2, the temperature was 120 °C and the feed concentration was 1.5 M benzoic acid in ethanol.

t_M Time the sample was measured	t_L Time the sample left the reactor	t_{In} Time the sample entered the reactor	τ Sample residence time	X Conversion	Outlet Concentration Benzoic Acid	Outlet Concentration Ethyl Benzoate
s	s	s	s	%	M	M
0	0	NA	NA	4.0	1.44	0.03
229	202	141	61	0.0	1.50	0.03
709	679	613	66	2.7	1.46	0.03
1189	1156	1084	72	2.7	1.46	0.03
1669	1632	1552	80	1.3	1.48	0.04
2089	2049	1960	88	2.7	1.46	0.04
2569	2523	2423	100	4.0	1.44	0.04
3049	2996	2880	115	5.3	1.42	0.05
3529	3465	3330	136	4.0	1.44	0.06
4009	3931	3766	164	4.0	1.44	0.07
4429	4331	4131	200	6.0	1.41	0.09
4909	4772	4512	260	7.3	1.39	0.11
5389	5168	4817	351	8.7	1.37	0.15
5869	5421	4979	442	16.7	1.25	0.17

Table S6. Time each sample was measured, left and entered the reactor and corresponding residence time, along with conversion and outlet concentrations of benzoic acid and ethyl benzoate for the Single-Variable Transient campaign. Initial flowrate was 100 µL/min, the flowrate was ramped down at a rate of 1 µL/min^2, the temperature was 140 °C and the feed concentration was 1.02 M benzoic acid in ethanol.

t_M Time the sample was measured	t_L Time the sample left the reactor	t_{In} Time the sample entered the reactor	τ Sample residence time	X Conversion	Outlet Concentration Benzoic Acid	Outlet Concentration Ethyl Benzoate
s	s	s	s	%	M	M
273	245	184	61	3.9	0.98	0.06
693	663	597	66	3.9	0.98	0.07
1173	1140	1068	72	4.9	0.97	0.07
1653	1617	1537	80	4.9	0.97	0.08
2133	2092	2003	89	5.9	0.96	0.09
2553	2507	2407	100	5.9	0.96	0.10
3033	2980	2865	115	6.9	0.95	0.11
3513	3450	3315	135	8.8	0.93	0.13
3993	3915	3752	163	10.8	0.91	0.16
4473	4372	4168	204	14.7	0.87	0.19
4893	4758	4500	258	17.7	0.84	0.24
5373	5157	4809	348	23.5	0.78	0.30
5853	5417	4977	440	29.4	0.72	0.34

11. Results from Two-Variable Transient Campaigns

The results obtained from the two-variable transient campaigns are shown in Table S7 and Table S8 for the "wide spacing" and "improved" experimental designs, along with time at which the measurement was taken, t_M, the time that the sample left the reactor outlet, t_L, the time the sample entered the reactor, t_{In}, and the sample residence time, τ. The temperature of the reactor at the time when the sample entered and left the reactor are also shown. The measured outlet concentrations along with the times the samples left the reactor were used for parameter estimation.

Table S7. Time each sample was measured, left and entered the reactor, corresponding residence time and the reactor temperature at the time the samples entered and left the reactor, along with conversion and outlet concentrations of benzoic acid and ethyl benzoate for the Two-Variable Transient "wide spacing" campaign. Initial flowrate was 100 µL/min, the flowrate was ramped down at a rate of 1 µL/min^2 and the temperature was ramped down from an initial temperature of 140 °C at a rate of 0.5 °C/min. The feed concentration was 1.50 M benzoic acid in ethanol.

t_M Time the sample was measured	t_L Time the sample left the reactor	t_{In} Time the sample entered the reactor	τ Sample residence time	T_{in} Reactor temperature at time t_{In}	T_L Reactor temperature at time t_L	X Conversion	Outlet Conc. Benzoic Acid	Outlet Conc. Ethyl Benzoate
s	s	s	s	°C	°C	%	M	M
73	46	NA	NA	140.0	139.6	8.0	1.38	0.09
553	524	460	64	136.2	135.6	6.0	1.41	0.07
1033	1001	931	70	132.2	131.7	4.0	1.44	0.07
1513	1478	1400	78	128.3	127.7	6.7	1.40	0.06
1933	1894	1809	85	124.9	124.2	3.3	1.45	0.05
2413	2369	2273	96	121.1	120.3	2.7	1.46	0.05
2893	2842	2732	110	117.2	116.3	2.0	1.47	0.04
3373	3313	3185	128	113.5	112.4	2.0	1.47	0.04
3853	3780	3626	154	109.8	108.5	4.0	1.44	0.03
4273	4183	3998	185	106.7	105.1	2.0	1.47	0.03
4753	4631	4394	238	103.4	101.4	2.7	1.46	0.03

Table S8. Time each sample was measured, left and entered the reactor, corresponding residence time and the reactor temperature at the time the samples entered and left the reactor, along with conversion and the outlet concentrations of benzoic acid and ethyl benzoate for the Two-Variable Transient "improved" campaign. Initial flowrate was 30 µL/min, the flowrate was ramped down at a rate of 0.25 µL/min^2 and the temperature was ramped down from an initial temperature of 140 °C at a rate of 0.2 °C/min. The feed concentration was 1.55 M benzoic acid in ethanol.

t_M Time the sample was measured	t_L Time the sample left the reactor	t_{In} Time the sample entered the reactor	τ Sample residence time	T_{in} Reactor temperature at time t_{In}	T_L Reactor temperature at time t_L	X Conversion	Outlet Conc. Benzoic Acid	Outlet Conc. Ethyl Benzoate
s	s	s	s	°C	°C	%	M	M
481	387	182	204	140.0	138.7	16.1	1.30	0.26
901	801	583	217	138.1	137.3	14.8	1.32	0.25
1321	1214	982	232	136.7	136.0	14.8	1.32	0.26
1741	1626	1377	248	135.4	134.6	14.8	1.32	0.24
2161	2036	1769	267	134.1	133.2	14.8	1.32	0.24
2581	2445	2157	289	132.8	131.8	14.8	1.32	0.24
3001	2852	2538	314	131.5	130.5	14.2	1.33	0.25
3421	3256	2913	344	130.3	129.1	14.2	1.33	0.25
3841	3657	3278	379	129.1	127.8	15.5	1.31	0.26
4261	4052	3631	421	127.9	126.5	15.5	1.31	0.26
4681	4440	3968	472	126.8	125.2	16.8	1.29	0.27
5101	4817	4283	534	125.7	123.9	17.4	1.28	0.28
5521	5177	4569	608	124.8	122.7	18.1	1.27	0.29
5941	5509	4815	694	123.9	121.6	20.0	1.24	0.30

References

1. Dortmund_Data_Bank, Dynamic Viscosity of Ethanol, http://www.ddbst.com/en/EED/PCP/VIS_C11.php).
2. Dortmund_Data_Bank, Density of Ethanol, http://www.ddbst.com/en/EED/PCP/DEN_C11.php).
3. Dortmund_Data_Bank, Liquid Dynamic Viscosity-Calculation by Vogel Equation, http://ddbonline.ddbst.de/VogelCalculation/VogelCalculationCGI.exe).
4. E. L. Cussler, *Diffusion: Mass Transfer in Fluid Systems*, Cambridge University Press, New York, 2009.
5. O. Levenspiel, *Chemical Reaction Engineering,* 3rd edn., Wiley, New York, 1999.
6. L. Falk and J.-M. Commenge, *Chem. Eng. Sci.*, 2010, **65**, 405-411.
7. R. K. Sinnott, in *Coulson and Richardson's Chemical Engineering,* 2nd edn., ed. R. K. Sinnott, Pergamon, Amsterdam, 1993, DOI: https://doi.org/10.1016/B978-0-08-041865-0.50020-9, pp. 565-702.
8. E. S. Domalski and E. D. Hearing, in *NIST Chemistry WebBook, NIST Standard Reference Database Number 69*, eds. P.J. Linstrom and W.G. Mallard, National Institute of Standards and Technology, Gaithersburg MD, 20899, 2018, DOI: http://doi.org/10.18434/T4M88Q, ch. Condensed Phase Heat Capacity Data.
9. R. W. Serth and T. Lestina, *Process Heat Transfer : Principles and Applications,* 2nd edn., Academic Press, Oxford, 2014.
10. L. Theodore, *Heat Transfer Applications for the Practicing Engineer*, John Wiley & Sons, Hoboken, NJ, 2011.
11. EngineeringToolBox, Thermal Conductivites for Some Common Liquids, https://www.engineeringtoolbox.com/thermal-conductivity-liquids-d_1260.html).
12. N.-S. Cheng, *Ind. Eng. Chem. Res.*, 2008, **47**, 3285-3288.
13. M. Righetti, G. Salvetti and E. Tombari, *Thermochim. Acta*, 1998, **316**, 193-195.
14. T. L. Bergman, F. P. Incropera, D. P. DeWitt and A. S. Lavine, *Fundamentals of Heat and Mass Transfer*, John Wiley & Sons, Hoboken, NJ, 2011.